Na 1*s* photoabsorption of free and deposited NaCl clusters: Development of bond length with cluster size

M. Riedler,[1] A. R. B. de Castro,[4] A. Kolmakov,[2] J. O. Löfken,[2] C. Nowak,[2] A. V. Soldatov,[3] A. Wark,[1] G. Yalovega,[3] and T. Möller[2,*]

[1]*II. Institut für Experimentalphysik, Universität Hamburg, Luruper Chaussee 149, D-22761 Hamburg, Germany*

[2]*Hamburger Synchrotronstrahlungslabor HASYLAB at Deutsches Elektronen Synchrotron DESY, Notkestrasse 85, D-22603 Hamburg, Germany*

[3]*Department of Solid State Physics, Rostov University, Sorge Street 5, 344102 Rostov-Don, Russia*

[4]*Laboratorio National de Luz Sincrotron, Campinas 13081-90, Brazil*

(Received 6 June 2001; published 6 December 2001)

Photoabsorption spectra of free and deposited NaCl clusters of up to 50 molecules are presented. The NaCl cluster films were produced using a method of cluster deposition. NaCl clusters covered with an Ar layer were produced by a pickup technique and then deposited on a cold gold substrate. Multiple-scattering oscillations in the Na *K*-edge absorption spectra allowed the determination of the bond length development of NaCl clusters with size. In addition, the spectra were compared with more advanced full-order multiple-scattering calculations. A comparison of the experimentally determined bond length with that calculated using a simple electrostatical model, assuming only a Coulomb interaction and a Born-Meyer-type repulsion of the ions, shows reasonable agreement.

DOI: 10.1103/PhysRevB.64.245419 PACS number(s): 78.70.Dm, 36.40.Mr, 61.10.Ht

I. INTRODUCTION

Clusters are small molecular aggregates which represent an intermediate case between atoms and macroscopic objects. During the last two decades, the investigation of the cluster size effects has become fundamental for our knowledge of the evolution of matter from the molecules to the solids. In addition, the discovery of the unusual physical and chemical properties of clusters has stimulated the broad applied research in the fields of micro- and optoelectronics, catalysis, and environmental science.[1]

Among the variety of experimental methods used for cluster research so far, x-ray absorption near-edge spectroscopy (XANES) is a very attractive one since it is sensitive to both the local geometrical and electronic structure around x-ray absorbing atoms.[2] In combination with intense sources for cluster beams, e.g., supersonic expansion and pickup sources,[3] it has been shown that this is a promising approach to investigate the size dependence of the electronic and geometrical properties of clusters in the gas phase. However, due to the diluted nature of the cluster targets in the gas phase, use of this method is limited. Therefore, the intensity limitations of the available cluster beams make it an attractive idea to collect clusters intact from the free beam inside an inert solid rare-gas media. Indeed, matrix isolation was one of the first techniques used to study physical and chemical properties of clusters.[4] In this case the electronic structure of the clusters is preserved due to the chemical inertness of rare-gas atoms and the coagulation of the particles is impeded by the low-diffusion coefficient inside the matrix. Up to now, several different experimental methods have been applied for the generation of matrix-isolated clusters, e.g., (i) codeposition of the clusters and the rare-gas beam,[5] (ii) deposition of the clusters onto a preadsorbed rare-gas buffer layer,[6] and (iii) deposition of atoms or molecules into the rare-gas matrix with subsequent controlled thermoactivated coagulation.[7] It should be emphasized that the use of the matrix-isolation approach ensures a weak interaction of the deposited cluster with the substrate and rare-gas matrix itself. Furthermore, the rare-gas matrix provides a transparent medium for electromagnetic radiation over a wide energy range. XANES and extended x-ray absorption fine structure (EXAFS) in conjunction with matrix isolation were already successfully used for the determination of the structure of metal clusters.[5,8–10]

For our experiments it was important to maintain the cluster size distribution in the cluster beam during the deposition of the clusters onto a substrate—i.e., to get a film consisting of well-isolated clusters with the same size distribution as in the gas phase. For the above-mentioned deposition techniques (i) and (ii), one has to consider fragmentation of the clusters during the deposition process and agglomeration due to surface diffusion on the substrate. Both create some uncertainty in the determination of the deposit cluster size. On the other hand, these two methods allow deposition of mass-selected clusters. The deposition of atoms or molecules and subsequent coagulation to clusters on the surface, as in method (iii), provides only a rough control concerning the final cluster size. In this article we present a method of cluster deposition. This method allowed us to determine experimentally a basic parameter like the bond length and its evolution with cluster size. The key idea of this approach is to deposit clusters, which are encapsulated inside a big rare-gas cluster. The principle of this method is schematically shown in Fig. 1. On the basis of the cluster formation process in the recently developed pickup cluster source,[3,11] it is possible to produce clusters of different materials embedded inside a host rare-gas cluster. The shell of rare-gas atoms around the guest cluster can be used to protect it against fragmentation and coagulation and agglomeration upon deposition onto a substrate. This method of cluster deposition preserves the

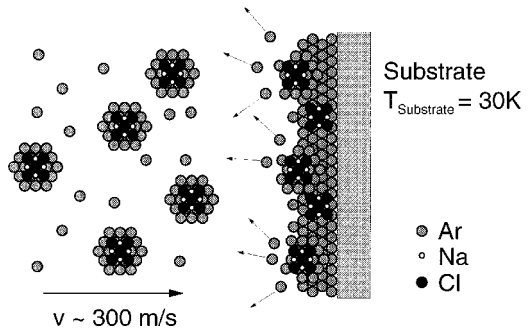

FIG. 1. Scheme of the deposition process of Ar-encapsulated NaCl clusters prepared by a pickup cluster source.

properties of the clusters in the gas phase inside the deposited matrix-isolated cluster film. Varying the number of picked-up molecules, the method provides the possibility to produce cluster films from different materials with controlled size distributions. Furthermore, with this deposition technique, it is possible to vary the thickness of the rare-gas shell around the core cluster. Also, modifications of the core cluster surface itself through the use of several materials in the pickup process are promising properties for future experiments. These advantages of the cluster deposition method give rise to a broad area of applications for different cluster film production.

We have applied this deposition technique to the system NaCl/Ar for two reasons: (i) The pickup of alkali-halide molecules by a host rare-gas cluster was recently intensively studied by mass spectroscopy[12,13] and in addition (ii) NaCl clusters have been investigated in great detail both experimentally[14,15] and theoretically,[16–21] providing a valuable background for the present research. The present investigation shows that NaCl clusters deposited in such a way exhibit a gradual evolution of the XANES features at the Na *K* edge with cluster size. We assign this behavior to the increase of the Na-Cl bond length with the increase of the mean cluster size. The bond length of Na-Cl inside the cluster could be determined quantitatively from the energy shift of the XANES features by using the interatomic-distance correlation function.[14]

A simple electrostatic model was applied to describe the evolution of the mean Na-Cl bond length together and of the mean binding energy with cluster size. Only the Coulomb interactions between the singly charged ions in the ionic bonded cluster and a repulsive Born-Meyer term were taken into account. As was already mentioned in the early work of Martin,[21] it is astonishing that this simple approach adequately describes the basic behavior of the bond length and the binding energy with cluster size in good agreement with more advanced calculations of the structure of NaCl clusters.[19,21] Because of the small computational demand, it is possible to calculate within this simple model the mean bond length and binding energies even for big clusters (in the present paper more than 35 000 atoms per cluster). This is an interesting size range, where the mean bond length of the cluster evolves from the molecular to the bulk value.

II. CALCULATION OF THE BINDING ENERGY AND BOND LENGTH

Several studies on the structure of neutral and charged NaCl clusters have been performed.[15,16,19–23] Since the binding in alkali-halide clusters has almost pure ionic character, the interaction potential between two ions can at first approximation be divided into a long-range classical electrostatic interaction and a quantum-mechanical short-range repulsive interaction. The simplest model, which describes ionic bonding, is the *rigid core model*:[21]

$$\Phi_{ij}=\frac{1}{4\pi\varepsilon_0}\frac{q_i\cdot q_j}{r_{ij}}+Ae^{-r_{ij}/\rho}, \tag{1}$$

where the first term is the Coulomb interaction between two point charges q_i and q_j separated by r_{ij}. The second term is the Born-Meyer term, which reflects the repulsion of ions due to the overlapping of wave functions. Assuming that the short-range interaction is effective only for nearest neighbors, the values for the two parameters A and ρ are given by $A=1.47\times10^{-16}$ J and $\rho=0.328$ Å.[22] This model does not consider charge-dipole and dipole-dipole interactions. Furthermore, it does not take into account the deformation of the electron distribution if two ions approach each other: i.e., the effective distance for the Born-Meyer interaction is different from r_{ij}. The more advanced *shell model* considers both effects by introducing a polarizability for each ion.[20] Comparison of these two models for neutral $(NaCl)_n$ and singly charged $[Na(NaCl)_n]^+$ clusters indicates that the simple rigid core model gives surprisingly good results in modeling the basic structure of these clusters.[21] However, it is necessary to emphasize that this is to a large extent peculiar to NaCl. For the heavier alkali halides, e.g., CsF, with a different size ratio and with elevated polarizability, there are remarkable differences in the structure calculated by the shell model and by the simplified rigid core model.[23]

The most favored structure for a given cluster size is found by minimization of the total energy. One of the standard techniques is simulated annealing. Within this method the ions are placed randomly in space and then the system is allowed to explore the potential energy surface while the total energy is slowly reduced. In principle, the system will end up in the global minimum. Unfortunately, for alkali-halide clusters this method is inefficient, because the energy surface has some deep local minima in it. Therefore, the process of simulated annealing has to be done slowly starting from high temperatures: i.e., it will take a long time for converging. Another common method for finding the global minimum is to start with a good intuitive guess of the structure of minimum energy and to find the closest minimum with a gradient descent optimizer.[20] Amara and Straub[16] used a quantum-mechanical annealing algorithm: the so-called adiabatic Gaussian density annealing (AGDA) optimization algorithm. The minimization takes place on an averaged potential, which is smoothed at high temperatures and rough at low temperatures.

The general structures found by these methods for NaCl clusters are confirmed by *ab initio* investigation.[19] Some deviations are found for small cluster sizes for metastable

structures. In the rigid core model, there are local minima for linear chains structures up to $n=6$ molecules, which are not predicted by the *ab initio* investigation already for the dimer. Furthermore, for small clusters up to $n\approx 20$, there is competition between two stable packings: either fragments of the solid, i.e., cubic, structure or hexagonal six-membered ring structure, which is not present in the solid. For cluster sizes $n>20$ the fcc-structure is dominant. Nevertheless, the most stable structure for a given NaCl cluster size is in good agreement within the simple rigid core or shell model and the *ab initio* calculations.

The above-mentioned calculations for NaCl cluster structures were made for $(\mathrm{NaCl})_n$ up to $n=32$, for $[\mathrm{Na(NaCl)}_n]^+$ up to $n=18$, and for $[(\mathrm{NaCl})_n\mathrm{Cl}]^-$ up to $n=35$. Of course, all of these methods have heavily increasing computational demand with increasing cluster size. Unfortunately, at present the calculation of basic parameters like bond length and binding energy for very big clusters can only be realized by exploiting simplified models with low computational demand. Therefore, we have used the rigid core model, Eq. (1), in conjunction with the concept of the Madelung number α for ionic crystals of the type A^+B^-.

The total lattice energy Φ of the cluster is simply the sum over all pair potentials Φ_{ij}. By expressing the distance r_{ij} as multiples p_{ij} of nearest-neighbor distances $\hat{r}$, i.e., $r_{ij}=p_{ij}\cdot\hat{r}$, and assuming that the repulsive Born-Meyer term is only effective for nearest neighbors, the total lattice energy Φ is given by

$$\Phi=\frac{e^2}{4\pi\varepsilon_0}\frac{1}{\hat{r}}\sum_i\sum_j\frac{\pm 1}{p_{ij}}+nA\langle\hat{z}\rangle e^{-\hat{r}/\rho}. \tag{2}$$

Furthermore, for each ion i of the cluster a Madelung number α_i is defined in the same way as for the bulk Madelung number by

$$\alpha_i=\sum_j\frac{\pm 1}{p_{ij}}. \tag{3}$$

For conventional reasons one takes the plus sign for attraction and the minus sign for repulsion in Eq. (3). The Madelung number α is only dependent on the geometrical structure. In contrast to the bulk, each ion of the cluster has a different geometrical environment because of the finite cluster size. Therefore, each ion has a different Madelung number α_i. Using Eq. (3), one gets for the lattice energy Φ of the cluster consisting of n molecules:

$$\Phi=-n\left(\langle\alpha\rangle\frac{e^2}{4\pi\varepsilon_0\cdot\hat{r}}-A\langle\hat{z}\rangle e^{-\hat{r}/\rho}\right), \tag{4}$$

where $\hat{r}$ is the nearest-neighbor distance, $\langle\hat{z}\rangle$ is the mean number of nearest neighbors, and $\langle\alpha\rangle$ is the mean Madelung number. For a given cluster size and geometry, one can calculate $\langle\alpha\rangle$ and $\langle\hat{z}\rangle$. In equilibrium conditions the lattice energy Φ [Eq. (4)] as a function of the nearest-neighbor distance $\hat{r}$ reaches a minimum:

$$\left(\frac{d\Phi}{d\hat{r}}\right)_{r_0}=0. \tag{5}$$

With this, one gets the mean nearest-neighbor distance r_0 and the mean bonding energy $E(r_0)$ per molecule for a given cluster. Comparison with experimental results and other theoretical methods has shown that this approach for NaCl clusters yields results in good agreement for bond length and binding energies as can be seen in Table I. One has to emphasize that within the frame of this model, one can only get mean values for bond length and binding energy. In fact, these values vary inside the cluster depending on the specific atom position; e.g., atoms at corner positions will be pulled inside and on the other hand facial atoms will be pushed out.[19] In our approach we assume cluster geometries that resemble a part of a perfect fcc lattice. The error made by this assumption will become smaller with cluster size, but also for small cluster sizes it is one of the favored structures. From this point of view, this simple method could be used to extend the cluster size range to bigger cluster sizes for comparison of experimental and theoretical results. Because of the simplicity, one can easily use this formalism for very big clusters–in the present paper the cluster consists of up to 35 000 atoms.

III. EXPERIMENT

The mixed clusters were prepared using a pickup method.[3] A primary argon cluster beam is produced by an adiabatic gas expansion through a conical nozzle (300 μm diameter, 8° opening angle) cooled to $T_{\mathrm{nozzle}}=80\,\mathrm{K}$. This rare-gas cluster beam passes through a skimmer into a scattering cell containing the vapor of sodium chloride. The molecules were picked up by the rare-gas cluster. Inside the parent cluster, the picked-up molecules coagulate and form an alkali-halide core cluster. By varying the parameters of the pickup process conditions, i.e., the degree of condensation, it was possible to produce not only NaCl clusters with different size distribution, but also embedded NaCl clusters within Ar host clusters. This process is controlled by the source parameters: pressure of the Ar gas at the nozzle ($p_{\mathrm{Ar}}=30$–$190\,\mathrm{mbar}$), temperature of the nozzle ($T_{\mathrm{nozzle}}=80\,\mathrm{K}$), and temperature of the oven ($T_{\mathrm{oven}}\leqslant 660\,^\circ\mathrm{C}$). For the subsequent cluster deposition, one has to choose the source parameters in such a way that one gets embedded clusters. The size distribution of the clusters in the gas phase before deposition is controlled separately by a time-of-flight reflectron mass spectrometer.

After completed cluster formation, the mixed clusters were deposited onto a gold-coated copper substrate cooled to $T_{\mathrm{substrate}}<30\,\mathrm{K}$. Due to the presence of a reasonable Ar gas component in the cluster beam, this deposition procedure can be considered to some extent as codeposition. In addition, the presence of the rare-gas shell around the core presumably prevents agglomeration of the NaCl clusters on the surface. Indeed, during the release of kinetic energy of the cluster upon deposition, some additional Ar atoms of the shell of the cluster will evaporate. Estimations of the kinetic energy of

TABLE I. Mean bond length $r_{\mathrm{expt,th}}$ and mean binding energy E_{th} per molecule for the NaCl molecule, NaCl clusters, and bulk NaCl resulting from our simplified model in comparison with more advanced theoretical calculations and other experimental results.

	Theoretical values		Experimental values		Present work	
Cluster	r_{th} [Å]	E_{th} [eV]	r_{expt} [Å]	E_{expt} [eV]	r_{th} [Å]	E_{th} [eV]
NaCl	2.27[a]	−5.420[a]	2.361[e]	−5.57[g]	2.264	−5.438
molecule	2.36–2.43[d]	−7.511[d]	2.388[f]			
$NaCl_2$	2.53–2.59[d]	−6.505[a]	2.500[e]		2.462	−6.553
dimer		−6.755[b]	2.584[f]			
		−7.511[d]				
	2.62–2.70[d]	−7.007[a]			2.589	−7.071
$(NaCl)_4$		−7.210[b]				
		−7.03[c]				
		−7.520[d]				
$Na(NaCl)_{13}$		−7.324[a]			2.683	−7.379
$3\times3\times3$		−7.394[b]				
		−7.03[c]				
$(NaCl)_{32}$	2.80[d]	−7.528[d]			2.717	−7.589
$4\times4\times4$						
$Na(NaCl)_{17968}$					2.801	−7.878
$33\times33\times33$						
NaCl			2.79[g]	−8.03[g]	2.811	−7.905
bulk						

[a]Reference 21.
[b]Reference 20.
[c]Reference 16.
[d]Reference 19.
[e]Reference 40.
[f]Reference 41.
[g]Reference 21.

our neutral clusters in the beam (velocity $v \approx 300$ m/s, i.e., $E_{\mathrm{kin}} = 19$ meV per Ar atom) versus the binding energy of a single Ar atom in the cluster (the binding energy per atom depends on the cluster size, e.g., $E_{\mathrm{dimer}} = 12.3$ meV in the dimer, $E_{N=55} = 53.3$ meV in an Ar_{55} cluster, and $E_{\mathrm{bulk}} = 88.8$ meV in the bulk) indicate that even for the case when the kinetic energy is totally transferred into desorption of Ar atoms only a minor fraction of the protective Ar shell will evaporate upon deposition.[24] As a result, Ar-encapsulated NaCl clusters together with the Ar gas component form an Ar matrix containing noncoagulated NaCl clusters. The mean NaCl cluster size and the Ar dilution ratio can be adjusted by varying the cluster source parameters. Because of these properties, we are able to prepare NaCl cluster films with different size distributions embedded in an Ar matrix by a single deposition process of mixed NaCl/Ar clusters.

The alkali-halide cluster films and free clusters in the gas phase were investigated by innershell photoabsorption spectroscopy. The experiments were performed at the high-resolution and high-flux undulator beamline BW3 (Ref. 25) (20–2000 eV) at HASYLAB at DESY. Monochromatized synchrotron light was used for a selective excitation of the Na 1*s* level (1070.8 eV). The Na *K*-edge absorption scans were recorded with time-of-flight (TOF) techniques, using the total yield of the photoelectrons (TEY) and the partial yield of the photoions (PIY, only free clusters). The partial pressure of the residual gas in the vacuum chamber was 10^{-8}–10^{-7} mbar. Therefore, the absorption spectra on deposited clusters were showing a degradation of the cluster-related signal already after approximately 5 min. To minimize the contamination of the matrix with the residual gas molecules, the geometry of the experiment was performed in such a way that simultaneous deposition and spectra acquisition were possible; i.e., the experiment was operated in a permanent deposition mode. A schematic view of the experimental setup is shown in Fig. 2.

Because of the random orientation of the isolated clusters,

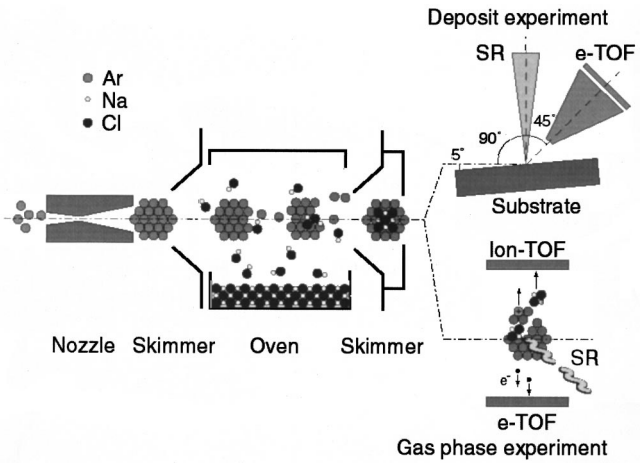

FIG. 2. Schematic view of the experimental setup. (a) Experiment on deposited clusters. (b) Experiment on gas phase clusters.

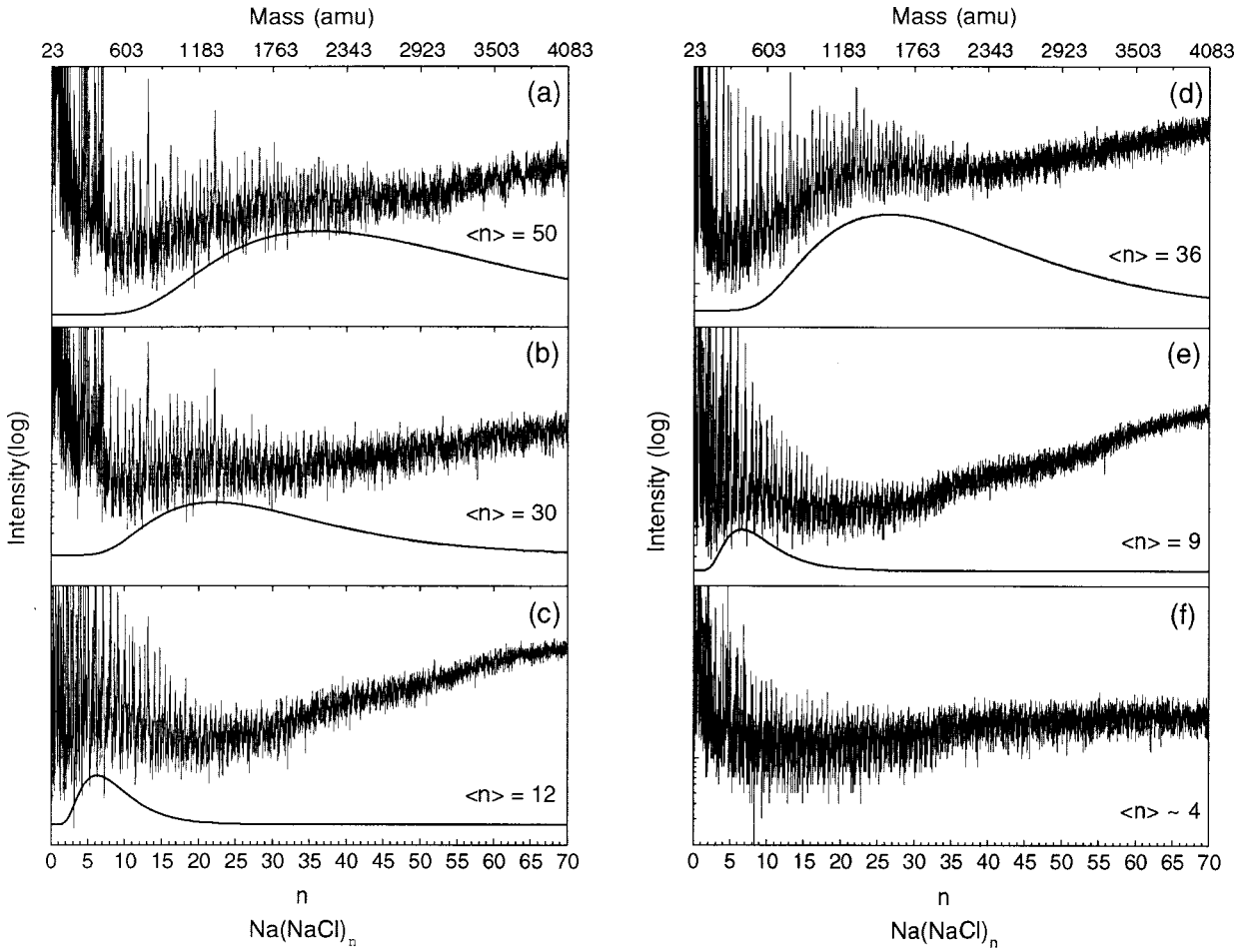

FIG. 3. Mass spectra of NaCl clusters which were used subsequently for absorption spectroscopy on deposited (spectra $a-c$) and gas phase clusters (spectra $d-f$). The size distribution is described by a log-normal distribution (solid curves). The width of the size distribution is given by $\sigma=0.5\langle n\rangle$.

we assume that the absorption spectra are rather independent of the angle of incidence of light. Therefore, this special geometry of the experimental setup should have no influence on the XANES spectra. Furthermore, even for solid NaCl crystals, no angle dependence was found.[26] During the absorption measurements, care was taken to stabilize the deposition conditions. The advantage of this method is that one always measures ''fresh'' samples. The deposition rate was chosen in such a way so as to minimize the charging of the sample. We do not observe any charging effects on XANES structures during spectra acquisition time (approximately 30 min). Our XANES spectra of solid NaCl are in good agreement with published results.[26]

IV. RESULTS

The cluster size distribution was determined with a reflection time-of-flight spectrometer. The mass spectra of the cluster size distributions, which were subsequently used for absorption spectroscopy, are shown in Fig. 3. Displayed is the logarithmic count rate of the reflectron mass spectrometer as a function of the mass of the detected particles. The sharp peaks of the bump in the lower-mass range in the mass spectra belong to nonstoichiometric $[Na_{n+1}Cl_n]^+$ clusters. These clusters are produced by ionization of stoichiometric NaCl clusters, through which one ionic-bonded Cl^- anion becomes neutral and desorbs from the remaining cluster. For that reason the mass unit for the lower x axis is converted into the cluster size n of $[Na_{n+1}Cl_n]^+$ clusters. The broad bump reflects the NaCl cluster size distribution in the mass spectra and is fitted with a log-normal distribution.[27] From this, one can determine the mean cluster size $\langle n\rangle$ and the standard deviation σ of the NaCl-cluster size. The additional bump at higher masses is due to Ar clusters.

We have prepared three different cluster size distributions for free clusters with mean size $\langle n\rangle=4$, 9, and 36 molecules and, respectively, $\langle n\rangle=12$, 30, and 50 molecules for deposit layers with a standard deviation of $\sigma=0.5\langle n\rangle$. Additionally, a solid NaCl sample was prepared by simple deposition of NaCl molecules at room temperature.

The Na *K*-edge absorption spectra on free and deposited NaCl clusters are shown in Fig. 4. In addition, the absorption of bulk NaCl and NaCl molecules was measured. The acquired spectra on solid NaCl films coincide with previously measured ones[26] from which the peak labeling was taken. For energy calibration the molecular spectra were measured simultaneously with the cluster spectra and the energy posi-

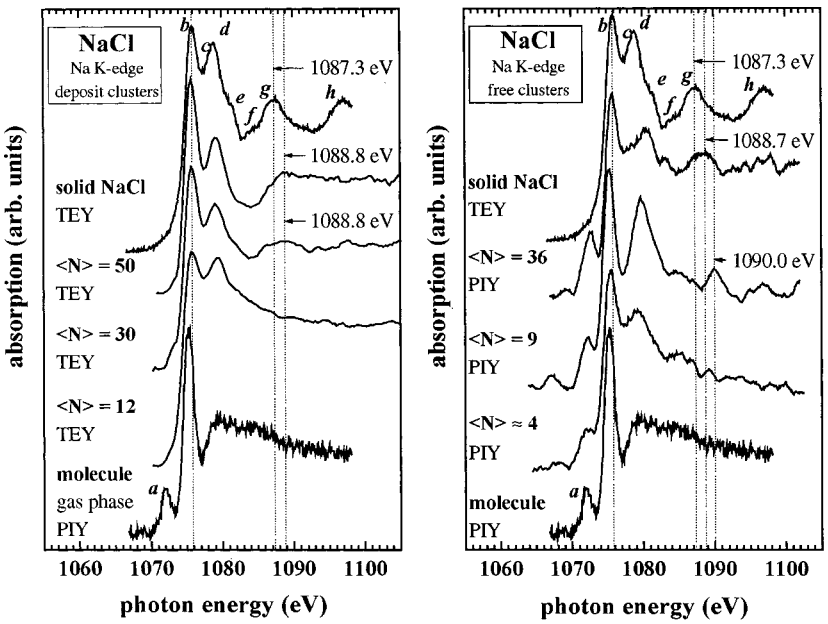

FIG. 4. Inner-shell photoabsorption spectra of deposited and gas phase NaCl clusters at the Na *K* edge. In addition, the absorption of bulk NaCl and NaCl molecules was measured. The energy position of the peak *g* was used for bond length determination (see text).

tion of peak *b* for the bulk spectra was aligned to the results of Kasrai *et al.*[14] We assume an error in the absolute energy of ± 0.5 eV. However, the error relative between different spectra is less than 1/10 eV.

A gradual development of the inner-shell absorption spectra with increasing cluster size towards the bulk spectra can be seen: namely, the variation in the near-edge structure and the development of higher-energy XANES structure as a function of cluster size. In addition, this fact demonstrates that there occurs no or little agglomeration of the NaCl clusters upon deposition inside the matrix. In the spectra of the smallest clusters, only the peaks *b* and *d* with similar intensity are seen. Furthermore, a small shoulder, labeled *a*, at the onset of the *K* absorption is observed. With increasing cluster size, the peaks *b* and *d* become more pronounced relative to the continuum background. However, an interpretation of the cluster size dependence of the intensity ratio between discrete and continuum states is difficult due to different fragmentation channels. Hereby, peak *b* becomes more intense than peak *d*. In addition, further XANES oscillations at higher energies develop and the spectra more and more resemble the solid-state spectra.

Sharp features near the threshold can be attributed to core-level excitons: i.e., an excitation of a core-level electron into an unoccupied bonded level. However, the identification of these peaks is not easy, because the exact energy position of the absorption edge is not known. Broader peaks above the threshold are attributed to photoelectron scattering resonances. These are well-known XANES features developing on the flat background due to the interference between the outgoing electron wave from the absorbing atom and the multiple-scattered electron waves at the surrounding atoms.[26]

V. DISCUSSION

There have been several studies of the near-edge structure of solid NaCl.[14,26,28,29] Fujikawa *et al.*[28] studied the Na *K*-edge XANES spectra of solid NaCl with short-range order full multiple-scattering calculations (MSC's) and could well describe the high-energy structures of the spectra (starting from peak *d*). Therefore, the first sharp feature in the absorption spectra peak *b*, which is not found in MSC's, can be associated to a localized transition from the $1s$ core level to the $3p$ state of Na^+. Hudson *et al.*[26] have simulated the solid XANES spectra with the curved-wave electron scattering code. They obtain good agreement for the broad high-energy peaks, too. But the origin of peak *d* as a photoelectron scattering resonance remains a matter of discussion. The XANES structure above peak *d* can be attributed to excitation of the electron into continuum states. However, there is still an uncertainty in the interpretation of the solid-state spectra. Cluster studies can provide valuable information on this issue. Indeed, the spectra of our smallest cluster size distributions has shown no structure above the peak *d*. And even for the bigger cluster sizes the higher-energy XANES features develop very slowly up to the solid spectra. The possible reason for this observation is a big fraction of surface atoms in the cluster, which therefore have less surrounding atoms for scattering the outgoing electron wave. On the other hand, even distant scatters contribute to the lower-energy XANES ($\approx$15 eV above threshold) of alkali halides. It is reported[26] that increasing the cluster size from 11 to 18 shells (179 to 389 atoms) gives an improved agreement in XANES structure calculations for solid NaCl. Therefore, it becomes clear why for our biggest cluster size, $\langle n \rangle = 50$ molecules, not all of the solid absorption features are present. To reassemble the solid spectra, the cluster size has to be increased further.

The main difference between the deposited and gas phase cluster absorption spectra is the behavior of the pre-edge structure *a*. This peak is present in the molecular spectrum, but only very weakly in our bulk spectrum (see Fig. 4). Murata *et al.*[29] assigned this structure to a ''forbidden'' $1s \rightarrow 3s$ transition, and it exhibits a temperature dependence in the absorption spectra of bulk NaCl. Therefore, the intensity

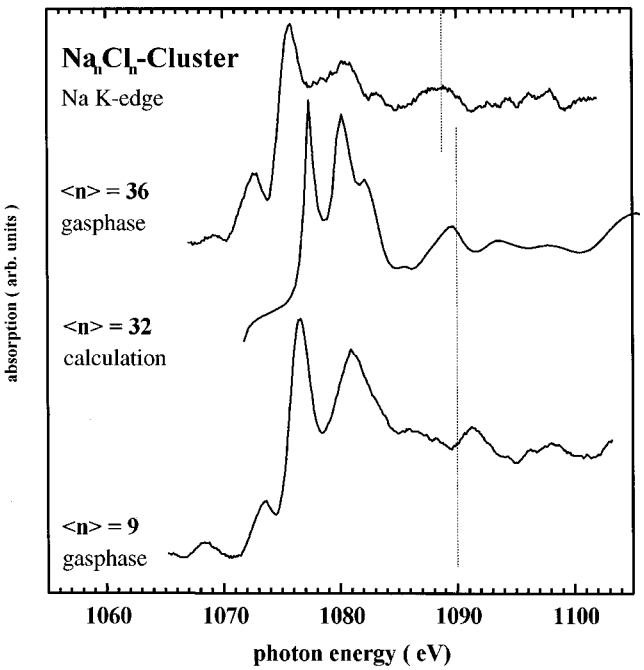

FIG. 5. Comparison of experimental and theoretical inner-shell absorption spectra on NaCl clusters at the Na *K* edge.

of the structure *a* increases with temperature. Absorption in bulk LiF at the Li *K* edge shows a similar structure below the absorption edge, which was assigned to a forbidden $1s \rightarrow 2s$ transition.[30,31] Also, experiments on other alkali halides, e.g., NaBr and KBr, exhibit such a structure *a* in the absorption spectra of molecules, but not or at least heavily reduced in the corresponding bulk spectra.[32] Federmann *et al.*[33] have shown that for Ne such forbidden transitions may be allowed at the surface of clusters. In NaCl cluster spectra (see Fig. 4), this structure *a* is seen for the gas phase clusters, but only weakly for the deposited clusters. This is probably due to the different surface composition of the NaCl clusters. Whereas the gas phase clusters have free surfaces the deposited clusters are embedded inside an Ar matrix.

Our main interest is the shift of peak *g* to smaller energies with increasing cluster size up to the bulk NaCl. This peak is well developed in the cluster spectra except for the smallest cluster sizes. The intensity of peak *h*, which should also show an energy shift with cluster size, is distinctly smaller in the gas phase spectra and for the deposited clusters not seen at all. This is in agreement with other experimental data on bulk NaCl (Refs. 14 and 26) and the theoretical calculations shown in Fig. 5. It is not quite clear to the authors why peak *h* has a similar intensity as peak *g* in our bulk spectra.

We assume that the energy shift of the peak *g* is due to the change of the Na-Cl bond length. The Na-Cl bond length in the molecule is given by $r_0 = 2.36$ Å and for the solid by $r_0 = 2.79$ Å.[21] Therefore, the bond length in a NaCl cluster should increase with size. A relation between the energy of an absorption peak E_r above the threshold and the distance *R* from the absorbing atom to a neighboring atom is given by Natoli:[34]

TABLE II. Determination of the nearest-neighbor distance r_0 in clusters as a function of size. The values for the energy position of the resonance peak E_r is taken from the absorption spectra shown in Fig. 4. Δ_g is the energy shift of the peak *g* in the cluster absorption spectra in comparison to the bulk energy position for different cluster size distribution $\langle n \rangle$. The energy $E_b = 1072.8$ eV was determined with Table III in Ref. 14. The calculation of the nearest-neighbor bond length r_0 is described in the text.

$\langle n \rangle$ [molecules per cluster]	E_r [eV]	Δ_g [eV]	$E_r - E_b$ [eV]	r_0 [Å]
50[a]	1088.8	1.5 ± 0.5	16.0	2.68 ± 0.05
36[b]	1088.7	1.4 ± 0.5	15.9	2.69 ± 0.05
30[a]	1088.8	1.5 ± 0.5	16.0	2.68 ± 0.05
9[b]	1090.0	2.7 ± 0.5	17.2	2.59 ± 0.05

[a]Deposited NaCl clusters.
[b]Free NaCl clusters.

$$(E_r - E_b) R^2 = C, \tag{6}$$

where E_b is the energy of a bound or excitonic resonance just before the edge, and *C* is a constant for the absorbing material. Kasrai *et al.*[14] applied this interatomic-distance correlation for several XANES spectra of solid alkali halides for the Cl *L* edge and the Na *K* edge. With their results for the bulk NaCl absorption spectra at the Na *K* edge [$E_b = 1072.84$ eV (Ref. 14)], we have determined the bond length r_0 in the clusters using Eq. (6) and the energy position $E_{r,\mathrm{cluster}}$ of peak *g* from our absorption spectra shown in Fig. 4:

$$r_0 = R_{\mathrm{bulk}} \sqrt{\frac{E_{r,\mathrm{bulk}} - E_b}{E_{r,\mathrm{cluster}} - E_b}}. \tag{7}$$

The results of this analysis of our absorption spectra from both deposited and free clusters are summarized in Table II. The error of the bond length r_0 (± 0.05 Å) is determined by the error of the binding energy E_b, which was assumed by ± 0.5 eV. For the smallest NaCl cluster sizes shown in Fig. 4, the multiple-scattering oscillation is scarcely developed. Therefore, a determination of the bond length r_0 for those cluster sizes was not possible.

Figure 5 shows a comparison between experimental gas phase spectra for $n = \langle 9 \rangle$ and $\langle 36 \rangle$ and a calculation for a cubic $Na_{32}Cl_{32}$ ($4 \times 4 \times 4$ atoms) cluster. The algorithm for the full multiple-scattering method used in this study has been previously described.[35,36] Recently, this algorithm has been also used to investigate the cluster geometry of $(NaCl)_4$ clusters.[37] For the calculation a muffin-tin (MT) potential with touching MT spheres has been constructed. The atomic charge densities have been obtained using the self-consistent solution of Dirac equation. The cluster of 64 atoms has cubic structure with Na-Cl bond distance equal to 2.7 Å. The structure of discrete states (peaks $a-d$) are strongly dependent on the choice of potential. Therefore, a comparison of these features between the experimental spectra and calculation is difficult. However, the XANES is well described by the full multiple-scattering method. The comparison of the structure *g* shows reasonable agreement between the experiment

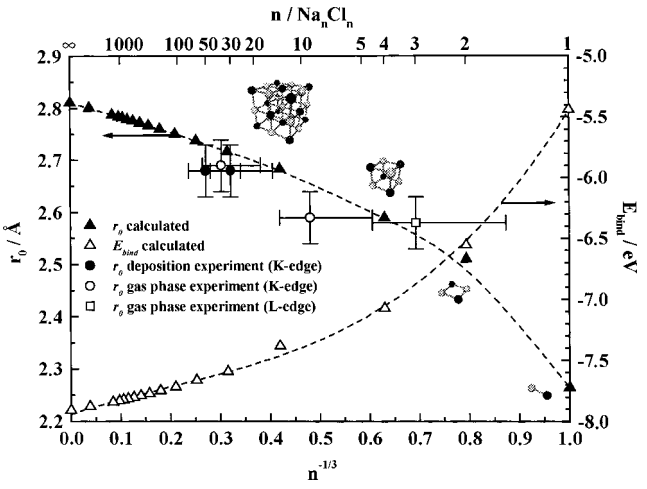

FIG. 6. Development of the mean bond length r_0 (solid triangles) and the mean binding energy E_b per molecule (open triangles) with cluster size obtained by our simplified model. The bond length is plotted vs $n^{-1/3}$, where n is the number of molecules per cluster. The experimental values for the bond length are plotted by open and solid circles. The additional experimental point for the $(NaCl)_3$ cluster was taken from Ref. 38. The dashed lines are plotted to guide the eye.

($\langle n\rangle = 36$) and the calculated spectrum ($\langle n\rangle = 32$), which indicates that our approach gives reliable results. Structures at higher energies around the energy position of the peak *h* in the bulk NaCl spectra (1097 eV) are seen with reduced intensity. This is in agreement with the fact that the peak *h* is scarcely or not seen in the cluster spectra, in contrast to peak *g*. The origin of the intense structure at around 1105 eV in the calculated spectra cannot be judged on the basis of our present research.

Another experimental value for the cluster size $n=3$ was obtained by XANES measurements on free clusters at the Cl $2p$ edge. The comparison of the measured spectra with theoretically predicted XANES spectra provided a bond length for the trimere of $r_0 = (2.58 \pm 0.05)$ Å.[38]

These values for the bond length for five different cluster sizes determined by the absorption spectroscopy of deposited and free NaCl clusters were compared with the simplified theoretical treatment described in Sec. II. In Fig. 6 the development of the calculated mean bond length $\langle r_0\rangle$ and the mean binding energy E_b per molecule with cluster size are shown for stoichiometric $(NaCl)_n$ and nonstoichiometric $[Na(NaCl)_n]$ clusters. The size range for the stoichiometric cluster is given from $n=2$ (dimer) to 864 ($12\times12\times12$ atoms) molecules. The nonstoichiometric clusters are displayed by half numbered n values from $n=13.5$ ($3\times3\times3$ atoms) to 17 968.5 ($33\times33\times33$ atoms); i.e., n is given by the number of atoms divided by 2. The bond length r_0 and binding energy E_b are plotted versus $n^{-1/3}$. Considering that the volume V of a cluster grows with the number of molecules n and the surface atomic fraction of the cluster is proportional to $n^{2/3}$, therefore $n^{-1/3}$ is given by the quotient of the number of surface atoms to the total number of atoms. Furthermore, one can imagine $n^{-1/3}$ as reciprocal to the ''radius'' of the whole cluster. In addition, this kind of display enables one to cover the whole size range from the molecule up to the solid state, i.e., between $n^{-1/3}=0$ and 1.

The experimental results for the bond length of deposited clusters for the mean cluster sizes $\langle n\rangle = 30$ and 50 as well as for the free NaCl clusters with mean cluster size $\langle n\rangle = 3$, 9, and 36 are shown in Fig. 6. As can be seen, the experimental and theoretical values are in good agreement. Therefore, the experimental results for the development of the bond length of NaCl clusters with size obtained from the energy shift of the resonance peak *g* are nicely verified by the applied simplified theoretical treatment. Further, we would like to point out that the bond length varies over a very large size range is due to the well-known slow convergence of the Madelung constant. On the other hand, the bond length of Na_4Cl_4, which is the smallest cubic structure, is almost exactly halfway between that of the NaCl molecule and bulk solid.

Hansen *et al.*[39] described the importance, for interatomic distance analysis, of thermal effects which influence the anharmonic motion of surface atoms. This gave rise to problems in bond length determination in the analysis of Cu clusters consisting of 100–1000 atoms. In this cluster size range, the variation of the bond length is small, and neglecting the temperature effect could give rise to a misinterpretation of the experimental data. In our present paper, we investigated much smaller clusters ($\langle n\rangle = 3-50$ molecules per cluster). In this size range, a large variation of the bond length r_0 is found. Furthermore, the anharmonic vibration of the surface atoms is important for room temperature and above. In experiments on both free and deposited clusters, the temperature of the clusters is far below room temperature. Therefore, in our case a temperature effect should only play a minor role.

VI. CONCLUSION

From the analysis of the development of XANES features of free and deposited NaCl clusters, the size dependence of the bond length was determined. The experiment on deposited clusters was realized with a modification of a cluster deposition technique where the deposition was made with Ar-encapsulated NaCl clusters. These heterogeneous clusters, which consist of a NaCl core cluster aggregated within an Ar parent cluster, were prepared with the pickup technique. The Ar shell prevents agglomeration of the NaCl clusters upon deposition. Finally, a cluster film is obtained where the intact NaCl clusters are embedded in an Ar matrix. Up to now our results have shown that these clusters preserve the original gas phase size distribution without observable coagulation on the surface upon deposition. Further measurements both in the gas phase and on deposits will be undertaken to clarify the deposition process and surface dynamics of these unusual clusters. Additionally, deposition of mass-selected clusters would improve the resolution of XANES spectra and therefore the development of the bond length with cluster size could be detected more accurately.

Finally, the experimental results were compared with a theoretical treatment of the size dependence of the bond length. In order to describe the bond length inside a cluster, even for very big clusters (number of molecules $n \approx 18\,000$),

we applied a simple theoretical model where only the Coulomb interaction and the Born-Meyer repulsive interaction between the ions inside the cluster were taken into account. This well-known *rigid core model* was combined with the concept of the Madelung number for ionic crystals. It was assumed that the clusters resemble a part of the fcc symmetry of the NaCl crystal. This simplified approach yields an astonishingly good agreement with other advanced theoretical models and experimental results. On the basis with only two parameters for the Born-Meyer repulsion (A,ρ) and the assumption of fcc symmetry, it becomes possible to describe the experimentally observed development of the bond length and the binding energy for the whole size range from the single molecule up to the solid state of NaCl.

ACKNOWLEDGMENTS

We gratefully acknowledge the financial support from the Deutsche Forschungsgemeinschaft under Grant No. SFB-508/C4 and Mo 719/1-3 as well as the cooperation of Russian scientists with support of the DFG under Grant No. DFG 436 RUS 113/241/2-1 and 2-2.

*Corresponding author.
Electronic address: thomas.moeller@desy.de

[1] H. Haberland, *Cluster of Atoms and Molecules* (Springer, Berlin, 1993).
[2] J. Stöhr, *NEXAFS Spectroscopy* (Springer, Berlin, 1992).
[3] M. Rutzen, S. Kakar, C. Rienecker, R. v. Pietrowski, and T. Möller, Z. Phys. D: At., Mol. Clusters **38**, 89 (1996).
[4] L. Andrews and M. Moskovits, *Chemistry and Physics of Matrix-Isolated Species* (North-Holland, Amsterdam, 1989).
[5] P. A. Montano, G. K. Shenoy, E. E. Alp, W. Schulze, and J. Urban, Phys. Rev. Lett. **56**, 2076 (1986).
[6] K. Bromann, C. Félix, H. Brune, W. Harbich, R. Monot, J. Buttet, and K. Kern, Science **274**, 956 (1996).
[7] P. S. Brechthold, U. Kettler, H. R. Schober, and W. Krasser, Z. Phys. D: At., Mol. Clusters **3**, 263 (1986).
[8] P. A. Montano, W. Schulze, B. Tesche, G. K. Shenoy, and T. I. Morrison, Phys. Rev. B **30**, 672 (1984).
[9] P. A. Montano, J. Zhao, M. Ramanathan, G. K. Shenoy, W. Schulze, and J. Urban, Chem. Phys. Lett. **164**, 126 (1989).
[10] H. Pudrum, P. A. Montano, G. K. Shenoy, and T. Morrison, Phys. Rev. B **25**, 4412 (1982).
[11] C. Rienecker, Ph.D. thesis, Universität Hamburg, 1998.
[12] A. Kolmakov, J. O. Löfken, C. Nowak, F. Picucci, M. Riedler, C. Rienecker, A. Wark, M. Wolff, and T. Möller, Eur. Phys. J. D **9**, 277 (1999).
[13] M. Wolff, Ph.D. thesis, Universität Hamburg, 1998.
[14] M. Kasrai, M. E. Fleet, G. M. Bancroft, K. H. Tan, and J. M. Chen, Phys. Rev. B **43**, 1763 (1991).
[15] J. P. K. Doye and D. J. Wales, Phys. Rev. B **59**, 2292 (1999).
[16] P. Amara and J. E. Straub, Phys. Rev. B **53**, 13 857 (1996).
[17] H. P. Cheng and U. Landmann, Science **260**, 1304 (1993).
[18] B. Sobelev, Phys. Solid State **35**, 1242 (1993).
[19] C. Ochsenfeld and R. Ahlrichs, J. Chem. Phys. **97**, 3487 (1992).
[20] N. G. Phillips, C. W. S. Conover, and L. A. Bloomfield, J. Chem. Phys. **94**, 4980 (1991).
[21] T. P. Martin, Phys. Rep. **95**, 167 (1983).
[22] T. P. Martin, J. Chem. Phys. **67**, 5207 (1977).
[23] J. Diefenbach and T. P. Martin, Surf. Sci. **156**, 234 (1985).
[24] M. Riedler, Ph.D. thesis, University Hamburg, 2000.
[25] C. Larsson, A. Beutler, O. Björneholm, F. Federmann, U. Hahn, A. Rieck, S. Verbin, and T. Möller, Nucl. Instrum. Methods Phys. Res. A **337**, 603 (1994).
[26] E. Hudson, E. Moler, Y. Zheng, S. Kellar, P. Heimann, Z. Hussain, and D. A. Shirley, Phys. Rev. B **49**, 3701 (1994).
[27] M. Lewerenz, B. Schilling, and J. P. Toennies, Chem. Phys. Lett. **206**, 381 (1993).
[28] T. Fujikawa, T. Okazawa, K. Yamasaki, J.-C. Tang, T. Murata, T. Matsukawa, and S.-i. Naoé, J. Phys. Soc. Jpn. **58**, 2952 (1989).
[29] T. Murata, T. Matsukawa, and S. Naoé, Solid State Commun. **66**, 787 (1988).
[30] B. F. Sonntag, Phys. Rev. B **9**, 3601 (1974).
[31] A. B. Kunz, J. C. Boisvert, and T. O. Woodruff, Phys. Rev. B **30**, 2158 (1984).
[32] A. Elafif, R. C. Karnatak, J. M. Esteva, C. M. Teodorescu, M. Womes, and E. Bouisset, Physica B **208&209**, 115 (1995).
[33] F. Federmann, O. Björnholm, A. Beutler, and T. Möller, Phys. Rev. Lett. **73**, 1549 (1994).
[34] C. R. Natoli, *EXAFS and Near Edge Structure* (Springer, Berlin, 1983), Vol. 27, p. 43.
[35] A. V. Soldatov, T. S. Ivanchenko, S. Della Longa, and A. Bianconi, Phys. Rev. B **47**, 16 155 (1993).
[36] S. Della Longa, A. V. Soldatov, M. Pompa, and A. Bianconi, Comput. Mater. Sci. **4**, 199 (1995).
[37] G. Yalovega, A. V. Soldatov, M. Riedler, A. Kolmakov, C. Nowak, and T. Möller (unpublished).
[38] C. Nowak, C. Rienecker, A. Kolmakov, J. O. Löfken, F. Picucci, M. Riedler, A. V. Soldatov, M. Wolff, and T. Möller, J. Electron Spectrosc. Relat. Phenom. **101-103**, 199 (1999).
[39] L. B. Hansen, P. Stoltze, J. K. Norskov, B. S. Clausen, and W. Niemann, Phys. Rev. Lett. **64**, 3155 (1990).
[40] P. A. Akischin, Z. Phys. Chem. (Leipzig) **213**, 111 (1960).
[41] R. J. Mawhorter, M. Fink, and J. G. Hartley, J. Chem. Phys. **83**, 4418 (1985).